

Cluster analysis of seriously injured occupants in motor vehicle crashes

Rocio Suarez-del Fueyo^{a,*}, Mirko Junge^b, Francisco Lopez-Valdes^c, H. Clay Gabler^d, Lucas Woerner^a, Stefan Hiermaier^e

^a Dr. Ing. h.c. F. Porsche AG, Germany

^b Volkswagen AG, Germany

^c Universidad Pontificia Comillas, Spain

^d Virginia Tech, USA¹

^e Albert-Ludwigs-Universität Freiburg, Germany



A B S T R A C T

Permanent monitoring of real-world crashes is important to identify injury patterns and injury mechanisms that still occur in the field despite existing regulations and consumer testing programs. This study investigates current injury patterns at the MAIS 3+ level in the accident environment without limiting the impact direction. The approach consisted of applying unsupervised clustering algorithms to NASS-CDS crash data in order to classify seriously injured, belted occupants into clusters based on injured body regions, biomechanical characteristics and crash severity. Injury patterns in each cluster were analyzed and associated with other characteristics of the crash, such as the collision configuration. The groups of seriously injured occupants found in this research contain a large amount of information and research possibilities. The resulting clusters represent new opportunities for vehicle safety, which have been highlighted in this study.

1. Introduction

In the late 1970s the National Highway Traffic Safety Administration (NHTSA) began publishing crashworthiness ratings of the most popular passenger vehicles sold in the United States (Hackney and Quarles, 1982). These ratings were based on the performance of the vehicle in pre-defined simulated crashes, in which Anthropomorphic Test Devices (ATD), or simply crash test dummies, mimicked the dynamic behavior of the human occupant and provided an estimation of the risk of injury to several body regions. Since then, vehicle safety regulations and consumer testing programs as well as improvements in road infrastructure have contributed to a substantial reduction of road traffic fatalities (Elvik et al., 2004; O'Neill, 2009; Glassbrenner, 2012; Kahane, 2015; van Ratingen et al., 2016). The continuous introduction and improvement of safety measures has always been based on the retrospective analysis of field data. Permanent monitoring of traffic crashes is essential to determine whether safety measures are effective to prevent injuries and fatalities in the real world. This evaluation can also identify injury patterns and injury mechanisms that still occur in the field despite current regulations and consumer testing programs. However, the analysis of accident data regarding injuries, injury severity and effectiveness of safety systems usually starts with filtering crashes by impact direction, similar to the approach of aforementioned crashworthiness

assessments (Brumberger and Zuby, 2009; Brumberger et al., 2015; Segui-Gomez et al., 2009, 2010). This initial filtering however potentially hinders finding injury patterns that are shared by crashes occurring under different impact directions.

In current crashworthiness assessments ATD loads, accelerations and deformations are compared to injury risk functions obtained experimentally to assess the risk of injury that the human occupant would sustain in a crash under similar conditions (Kleinberger et al., 1998). These injury criteria are capable, in some instances, to discriminate between different injury severity levels. The Abbreviated Injury Scale (AIS) classifies the severity of injuries according to their life-threatening consequences. The AIS is an ordinal, non-linear, 1 through 6 scale, in which serious injuries receive a score of 3 or higher (AIS 3+) (AAAM, 2008; Segui-Gomez and Lopez-Valdes, 2012). Occupant restraint systems are developed to minimize the probability of sustaining a serious injury to a specific body region, p(AIS 3+), as measured by crash test dummies. Modern ATDs, such as the THOR-50M and the World-SID dummies, may help by predicting injury to body regions and in impact directions not possible with earlier dummies (Rhule et al., 2009; Parent et al., 2017). There is however a substantial body of literature pointing to the limitations of these mechanical devices to adequately mimic the human behavior (Seacrist et al., 2010; Lopez-Valdes et al., 2010, 2019). Furthermore, ATDs are directional, namely, there are specific ATDs for

* Corresponding author.

E-mail address: rocio.suarez.del.fueyo@porsche.de (R. Suarez-del Fueyo).

¹ <https://beam.vt.edu/people/faculty/gabler.html>

frontal, side or rear impacts. Likewise, their associated injury criteria are also limited to specific directions. This characteristic of the ATDs has motivated a number of studies that have investigated the injury risk to different body regions for particular collision configurations, or have focused on the evaluation of safety systems addressing only certain collision configurations (Stigson et al., 2012; Brumbelow, 2019; Crandall et al., 2001).

In addition to the aforementioned, many descriptive studies of real-world crash data have focused on MAIS 2+ injured occupants due to the reduced number of severe crashes in accident databases (Forman et al., 2019; Andricic et al., 2018), while crashworthiness assessments have the objective to address MAIS 3+ injuries.

The current study proposes a new approach to explore the entire accident environment applying unsupervised clustering algorithms to real-world crash data. Seriously injured occupants are classified into clusters based on injury patterns at the MAIS 3+ level, biomechanical characteristics of the occupants and crash severity, without limiting the impact direction. The goal is then to identify the injury patterns of the occupants in the same cluster and associate them with other conditions of the crash, such as the collision configuration. This is the first study applying unsupervised clustering techniques to accident data in order to determine potential improvements in vehicle safety by identifying MAIS 3+ injury patterns without limiting impact direction.

2. Materials and methods

2.1. Data set

The National Automotive Sampling System – Crashworthiness Data System (NASS-CDS) investigated until 2015 up to 5000 statistically selected crashes per year in the US. Information about the accident scenes, the vehicles involved in the crash and the injured occupants was collected, examined and introduced in the data base (Zhang and Chen, 2013; Radja, 2016). In this study, real-world crash data from NASS-CDS between the years 2000 and 2015 was analyzed. Front row occupants of passenger vehicles were considered. Only occupants aged 16-years and older were considered due to the biomechanical differences between adults and children (Arbogast et al., 2005). Being restrained by a 3-point-belt was a further inclusion criterion. In order to consider modern vehicles for the study and at the same time count with a significant amount of data, only occupants in vehicles with model year from 2000 and later were considered. In 2009 NHTSA stopped collecting medical information of occupants of vehicles that were older than 10 years at the time of the accident (NHTSA, 2019). These cases were therefore not included. Rollover crashes were excluded from the data sample. NASS-CDS weights have not been used in this study.

2.2. Body regions, injury aggregation and injury severity

Injury severity in motor vehicle crashes can be described with different injury metrics (Gabler et al., 2015). AIS classifies injuries on an ordinal scale from 1 to 6, which basically represents the threat of life associated with the injury (AAAM, 1998, 2008). In this study, injury severity levels were assessed using the AIS98 codes (AAAM, 1998). Occupants were selected for the research if they were MAIS 3+ injured or if they sustained at least three AIS 2 injuries. Injury patterns were examined within the body regions head, face and neck (HFN); thorax and thoracic spine (THO); abdomen and lumbar spine (ABD) and knee, thigh and hip (KTH). Occupants who sustained a MAIS 3+ injury to a single body region not included within the four considered were included in the sample but not examined in the further analysis of the clusters.

The New Injury Severity Score (NISS), similar to the Injury Severity Score (ISS), is also an AIS-based scale for trauma severity. This score focuses on the AIS codes of the three most severe injuries (Baker et al., 1974; Osler et al., 1997). In the current analysis the injury severity of the

body regions was also aggregated using the AIS codes in much of the same way as the NISS: the injury severity of a body region is represented by the three most severe injuries to that body region.

Because the performed clustering algorithm could not use categorical variables, the AIS code was rescaled in order to transform the NISS scale into a metric scale with respect to mortality (Stevens, 1946) Niebuhr et al. proposed the AISx, a transformation of the AIS scale, for rescaling the ordinal AIS scale to an interval scale (Niebuhr et al., 2013, 2015, 2016). Using AISx to calculate NISS-like body region specific injury severities results in the needed metric measure, the NISSx. (Eq. (1)). This exponential transformation is injective and linearizes the AIS scale with respect to lethality (Gaylor et al., 2016). The NISSx can be calculated as the sum of the respective AISx, as presented in Eq. (2). The index i refers to the first, second or third highest AIS score of a given body region:

$$\text{AISx}_{[i]} = 25 \cdot \frac{(e^{\text{AIS}_{[i]}} - 1)}{(e^5 - 1)} \quad (1)$$

$$\text{NISSx} = \sum_{i=1}^3 \text{AISx}_{[i]} \quad (2)$$

In order to simplify the results and focus on the severely injured body regions, the injury severity level of the four considered body regions was divided into three categories, MAIS 0–1, MAIS 2 and MAIS 3+, after the cluster analysis.

2.3. Clustering algorithm

Using machine learning algorithms, an automated cluster analysis was performed on nine variables of the data set. The variables of the clustering model included the injury severity to the four main body regions (HFN, THO, ABD and KTH), occupant age, body mass index (BMI), change of velocity during the crash (delta v), mass ratio (MR) of the collision participants and model year of the case vehicle. As mentioned above, the NISSx score was used as a measure of the injury severity of each body region in the cluster analysis. Occupant age was included to take into account a reduced injury tolerance with aging (Kent et al., 2005). The mass ratio (calculated as shown in Eq. (3)) was used to consider the mass-compatibility between the case vehicle and the collision partner. The model year of the case vehicle was also included in the model. Delta-v is the absolute value of the momentum change the vehicle was exposed to. All cases, in which the aforementioned variables were missing or unknown were excluded from the data sample. All variables in the model are quantitative variables. With this data model, where each data point is a MAIS 3+ injured occupant, the clustering algorithm was performed:

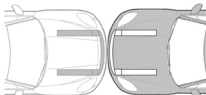
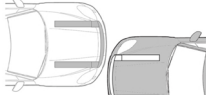
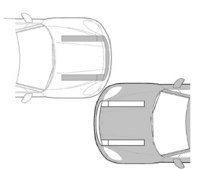
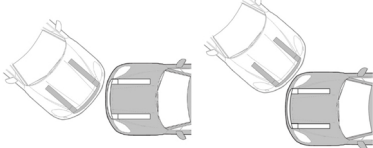
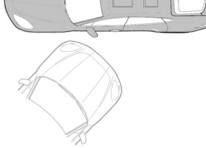
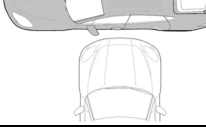
$$\text{MR} = \frac{m_{\text{partner}}}{m_{\text{case}}} \quad (3)$$

The clustering algorithm consists of two steps. First, principal component analysis (PCA) was performed with the data (Pearson, 1901). Thereafter, K-means clustering was applied (MacQueen, 1967).

PCA summarizes the information of a data set containing multiple correlated quantitative variables. PCA extracts the important information in a data set and expresses this information as a set of a few variables called principal components (PC). The dimension reduction is achieved by identifying the principal directions in which the data varies and the principal components correspond to a linear combination of the original variables (Pearson, 1901). PCA was performed with the package *factoextra* (version 1.0.5) in the R statistical software (version 3.5.2). The variables of the model were normalized before applying PCA, i.e. all variables were transformed into variables with mean 0 and standard deviation 1. Each variable in the model represents one dimension. The main results of the PCA are presented in Table 4 in Appendix A. For the subsequent analysis, the principal components PC1 to PC6, describing

Table 1

Collision configuration classification. Frontal collisions are classified based on Brumbelow (2019). Different collision configurations as those presented here are classified into the category *Other*.

Collision type	Collision configuration	Example
Frontal	Large overlap – axial loading of both longitudinals	
	Moderate overlap – axial loading of one longitudinal	
	Small overlap – axial loading outboard of longitudinals	
	Frontal oblique – oblique loading of both or only one longitudinal	
Lateral	Lateral oblique – oblique loading of the passenger compartment region	
	Lateral 90° – perpendicular loading of the compartment region	

77% of the variance of the data (see Table 4) were considered. So, the data model was reduced from nine to six dimensions.

After the dimension reduction with PCA, K-means clustering was performed with the *Package stats* in R. K-means is one of the most frequently used unsupervised machine learning algorithms (MacQueen, 1967). K-means classifies the data points into groups (i.e. clusters) so that the within-cluster variation is minimized. Each cluster is defined by its centroid, which corresponds to the mean of the data points in each cluster. K-means starts with a number (k) of randomly selected centroids and performs iterative calculations to optimize the position of the centroids. The algorithm used in this study was the Hartigan and Wong algorithm. The authors defined the total-within cluster variation as the sum of squared distances (Euclidean distances) between each data point (x_i) and its corresponding centroid (μ_k) of the cluster (C_k), as in Eq. (4) (Hartigan and Wong, 1979; Kassambara, 2017).

$$W(C_k) = \sum_{x_i \in C_k} (x_i - \mu_k)^2 \quad (4)$$

K-means algorithm requires the number of clusters K to perform the clustering. Finding the appropriate number of clusters requires trading off between few number of clusters and a small total within-clusters sum of squares (SST). The elbow method was used to estimate the

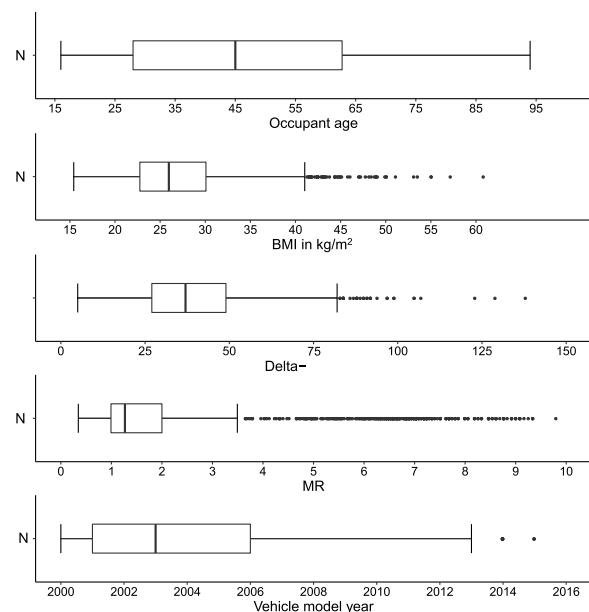


Fig. 1. Descriptive statistics on the data sample ($N = 1350$).

recommended number of clusters. The idea of the elbow method is to run K-means clustering for a number of K clusters, calculate the total sum of squares within the clusters for each value of k (each cluster) as indicated in Eq. (5), and then plot a line graph as shown in Fig. 14 in Appendix A. If the line chart looks like an arm, then the “elbow” is the recommended value of K , since from that point on the variance starts to have diminishing values by increasing K (Kodinariya and Makwana, 2013):

$$SST = \sum_{k=1}^K W(C_k) = \sum_{k=1}^K \sum_{x_i \in C_k} (x_i - \mu_k)^2 \quad (5)$$

In this case, K-means clustering was computed with $K = 2$ to $K = 12$. The SST values corresponding to the number of clusters were calculated and represented in Fig. 14 in Appendix A. The arm shape of the line chart can be seen and a bend or “elbow” can be observed at $K = 6$. Thus, the injured occupants meeting the inclusion criteria were automatically grouped in 6 clusters.

2.3.1. Analysis of the clusters

Each seriously injured occupant in the sample was assigned to one of the six clusters. At this stage, the data set and each cluster were examined regarding the input variables, in particular the most frequent injury patterns within the four body regions. For each data point, all variables recorded in NASS-CDS are still known and can be analyzed, even though they were not included in the clustering model. Subsequently, other relevant information related to the crash was examined in an attempt to match the clusters to specific crash circumstances (information not included in the clustering algorithm), such as the collision configuration.

Photographs of all the case vehicles in the sample were reviewed in order to assign a collision configuration based on the structural deformation similarly to Brumbelow (2019) (Brumbelow and Zuby, 2009; Brumbelow, 2019). In the frontal configurations the distinction was done by analyzing whether the loading was collinear or oblique to the longitudinals, designed to absorb energy in collinear direction, and whether the longitudinals had experienced deformation or not. In the case of the lateral collisions, it was only determined, whether the main impact zone was located in the zone of the passenger compartment or outboard the passenger compartment. The classification of the collision configurations is shown in Table 1. Additionally, the collision opponent was analyzed and classified in different categories depending whether it

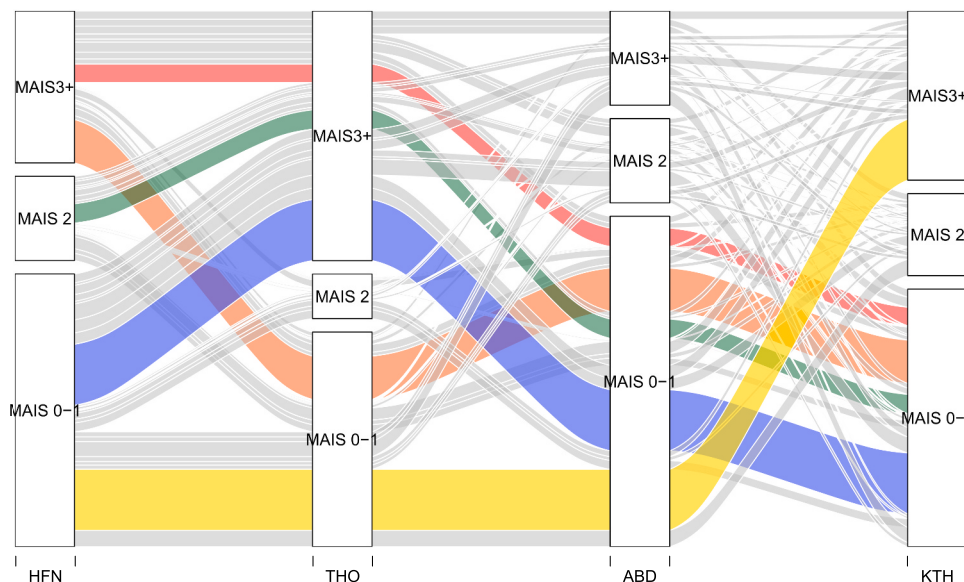


Fig. 2. Body region based injury patterns of seriously injured belted front row car occupants in the data sample. Three levels of injury severity: MAIS 0–1, MAIS 2 and MAIS 3+. The size of the injury severity boxes and the width of the connecting curves are proportional to their frequency in the sample (HFN: Head-Face-Neck, THO: Thorax, ABD: Abdomen, KTH: Knee-Thigh-Hip). For interpretation of the references to color in this figure citation, the reader is referred to the web version of this article.

was an object or a vehicle, and if a vehicle, by its body type.

3. Results

The sample included 1350 seriously injured occupants. Data in the sample were analyzed with regard to the nine clustering variables, in order to be able to compare the information grouped into the clusters to the whole sample. Fig. 1 shows descriptive statistics on the age distribution of the occupants, BMI, delta-v, MR of the collision, and vehicle model year in the data set. As shown in these box-plots, the age of the occupants is nearly homogeneously distributed within the data sample: The median age is 45 years of age, and 25% of the occupants are older than 63 years. The BMI of half of the passengers is below 26 kg/m², which is considered to be a healthy weight. For a quarter of the occupants the BMI is higher than 30 kg/m² (moderately to severely obese). The 75th percentile of the delta-v distribution corresponds to 50 km/h, inferring that the crashes in the data sample do not differ from the current crashworthiness assessments in crash severity. The median MR is 1.3, which reveals that most of the collisions in the clusters were passenger vehicle-to-passenger vehicle crashes, with the case vehicle being lighter than the collision partner. The MR outliers represent the crashes in which the collision partner was much heavier than the case vehicle or the crashes against rigid objects. The distribution of the vehicle model year shows that the 50% of the vehicles in the sample correspond to the model years between 2001 and 2006. 25% of the vehicles are newer than 2006.

The body regions based injury patterns of the occupants in the data sample are presented in Fig. 2. Each column of the chart represents one body region (HFN: Head-Face-Neck, THO: Thorax, ABD: Abdomen, KTH: Knee-Thigh-Hip). Columns are subdivided into three blocks, indicating the injury severity level (MAIS 0–1, MAIS 2 and MAIS 3+), sized to their relative frequencies. MAIS 3+ thoracic injuries (the largest MAIS 3+ block), followed by KTH and HFN MAIS 3+ injuries, were the most frequent serious injuries in the sample. The injury patterns are indicated with curvy lines which connect the injury severity levels of the four body regions. The width of the lines is proportional to the frequency of the injury pattern in the sample. When an injury pattern was sustained by 40 or more occupants, the corresponding curvy line was highlighted in a different color than gray. The most prevalent injury patterns in the data sample are displayed in blue, yellow, orange, red and dark green. The blue line shows the occupants who only sustained a MAIS 3+ injury

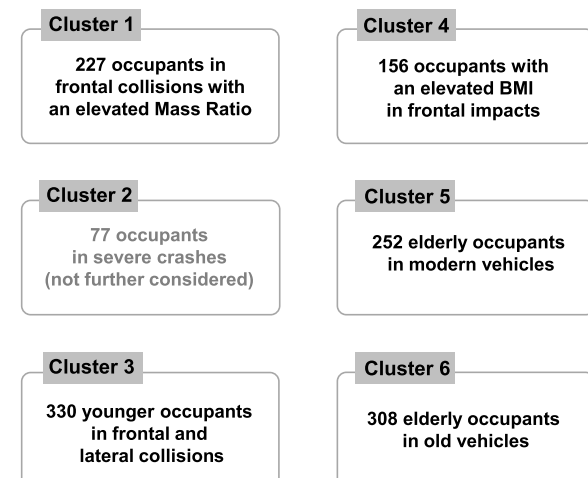


Fig. 3. Clusters of seriously injured occupants. Summary of the results.

to the thoracic region. The orange and yellow curves also indicate a single MAIS 3+ injured body region. The yellow one indicates serious knee-thigh-hip injuries and the orange one shows serious head-face-neck injuries. The red curve indicates the proportion of occupants with MAIS 3+ injuries to the HFN and THO regions. Occupants who sustained a MAIS 2 injury to the head and a MAIS 3+ injury to the thorax are indicated by the dark green curvy line. The gray curves indicate other less prevalent injury patterns in the data sample.

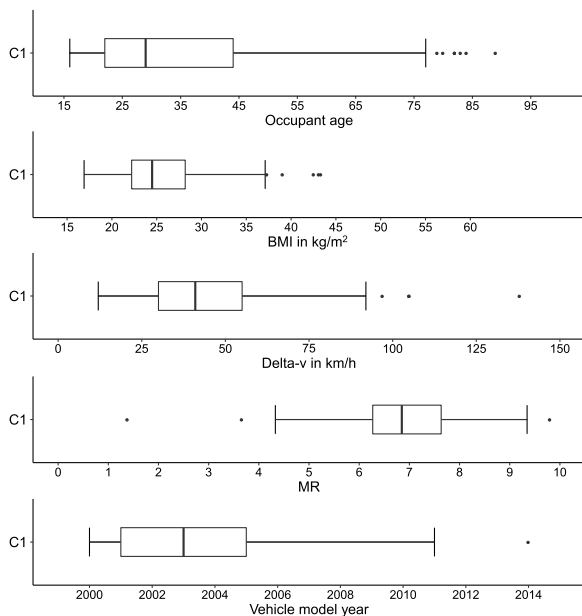
Table 2
Collision configurations in the data sample and within the clusters.

Collision configuration	Data sample (%)	Cluster					
		1 (%)	2 (%)	3 (%)	4 (%)	5 (%)	6 (%)
Large overlap	19	18	18	21	25	22	12
Moderate overlap	14	25	13	10	15	15	9
Small overlap	5	10	0	4	8	4	4
Frontal oblique	24	13	9	20	22	30	37
Lateral oblique	19	9	44	26	16	13	22
Lateral 90	9	9	9	12	8	4	10
Other	10	16	7	7	6	12	6

Table 3

Type of collision opponent in the data sample and within the clusters.

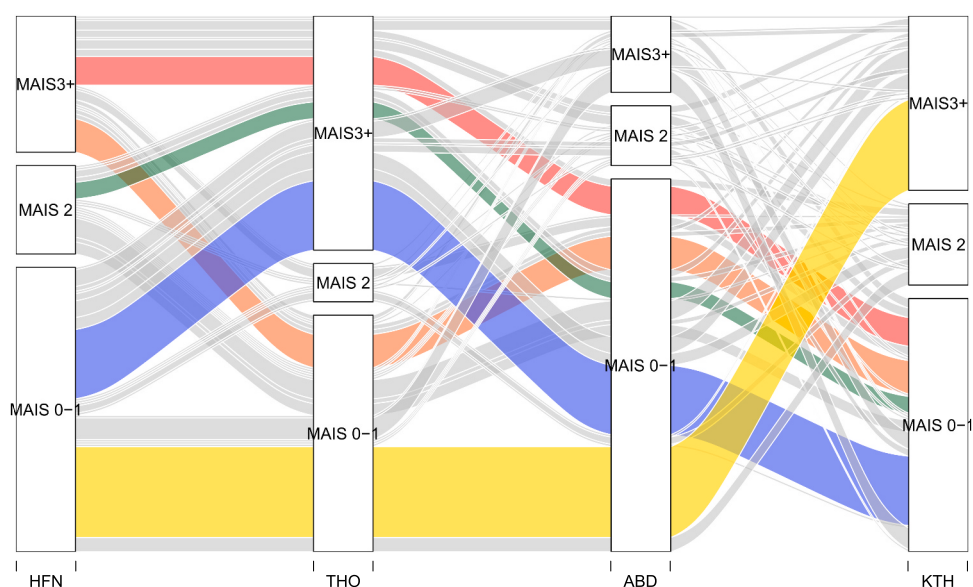
Collision opponent	Data sample (%)	Cluster					
		1 (%)	2 (%)	3 (%)	4 (%)	5 (%)	6 (%)
Car	36	0	29	43	48	45	43
SUV / Pick-up	34	1	44	45	30	42	41
Van	7	0	9	9	6	6	10
Wall-type object	3	13	1	1	1	2	1
Pole-type object	17	73	9	2	10	5	4
Other object	3	13	8	0	5	0	1

**Fig. 4.** Descriptive statistics of the model variables in cluster 1 (C1 = 227).

The clustering algorithm identified six clusters describing 77% of the sample variability (Table 4). Each seriously injured occupant was assigned to only one group. The clusters were analyzed regarding the clustering variables in order to understand what kind of information was associated with each group of data (Figs. 4–13). The resulting clusters, named after its main characteristics and indicating the number of associated occupants, are shown in Fig. 3. Cluster 3 and cluster 6 are the largest clusters with 330 and 308 occupants. Clusters 5, 1 and 4 follow with 252, 227 and 156 data points respectively. Cluster 2 is the smallest cluster with only 77 cases. Since this cluster only includes catastrophic crashes with a high delta-v, it was not further considered for a more comprehensive analysis. The associated collision configurations with the clusters were analyzed and classified as shown in Table 1. The results are listed in Table 2. The type of the collision opponent corresponding to the crashes in the clusters are represented in Table 3.

3.1. Cluster 1

Descriptive statistics of cluster 1 are shown in Fig. 4. The median occupant age in the cluster is 29 years and 75% of the occupants are younger than 44 years of age. The median BMI of the cluster is approximately 25 kg/m². The 75th percentile of delta-v corresponds to 55 km/h. The variable model year is distributed similarly as in the data sample. The increased MR is the principal characteristic of this cluster, which reveals a mass incompatibility issue. As shown in Table 3, over 70% of the cases occurred against a pole-type object. In Fig. 5 two predominant injury patterns can be distinguished. In most cases the occupants sustained a MAIS 3+ injury to the KTH region (yellow), following by the occupants who sustained a severe injury to the thorax as a single injury (blue). Cases with both HFN and THO regions being severely injured are also prevalent in this cluster (red). Other injury patterns which were categorized as frequent in the whole sample are highlighted in orange and dark green. Less frequent injury patterns are colored in gray. Results in Table 2 indicate that the most common collision configuration in cluster 1 was frontal impact with moderate overlap, followed by large overlap frontal collisions. The high proportion of small overlaps compared to the other clusters is noticeable.

**Fig. 5.** Body region based injury patterns of seriously injured belted front row car occupants in cluster 1. Three levels of injury severity: MAIS 0–1, MAIS 2 and MAIS 3+. The size of the injury severity boxes and the width of the connecting curves are proportional to their frequency in cluster 1 (HFN: Head-Face-Neck, THO: Thorax, ABD: Abdomen, KTH: Knee-Thigh-Hip). For interpretation of the references to color in this figure citation, the reader is referred to the web version of this article.

3.2. Cluster 3

The results of the descriptive analysis for cluster 3 are shown in Fig. 6. 75 % of the occupants are younger than 38 years old. Cluster 3 is the cluster of the young population. The median BMI corresponds to 23 kg/m^2 . 50% of the crashes had a delta-v between 33 and 53 km/h. The MR is concentrated between 1 and 1.5 and the case vehicles in this cluster are older when compared to the data sample. Fig. 7 illustrates that MAIS 3+ injuries to the head, thorax and KTH region are almost equally frequent in this cluster. Most of the occupants sustained a MAIS 3+ injury to the KTH region as the single injury (yellow), followed by the occupants who sustained a severe injury to the head (orange) and the ones who were severely injured in the head and the thorax (red). Other injury patterns in common with the whole sample are also highlighted in Fig. 7 (blue, dark green).

Table 2 shows a similar distribution between

lateral oblique, frontal oblique and large overlap frontal crashes.

3.3. Cluster 4

The elevated BMI with approximately 36 kg/m^2 as the 50th percentile and 42 kg/m^2 as the 75th makes cluster 4 the cluster of the obese occupants. This evidence is presented in Fig. 8. Age is equally distributed across all age groups. Delta v and MR are comparable to the distributions of the data sample. Case vehicles in cluster 4 are slightly newer compared to the sample. MAIS 3+ injuries in the KTH region as single injury are clearly the most prevalent injury pattern in cluster 4, as highlighted in yellow in Fig. 9. This injury pattern may be related to the high BMI of the occupants. Injury patterns in common with the other clusters are also highlighted in the plot. The corresponding collision configurations are indicated in Table 2. Full frontal crashes (25%) and

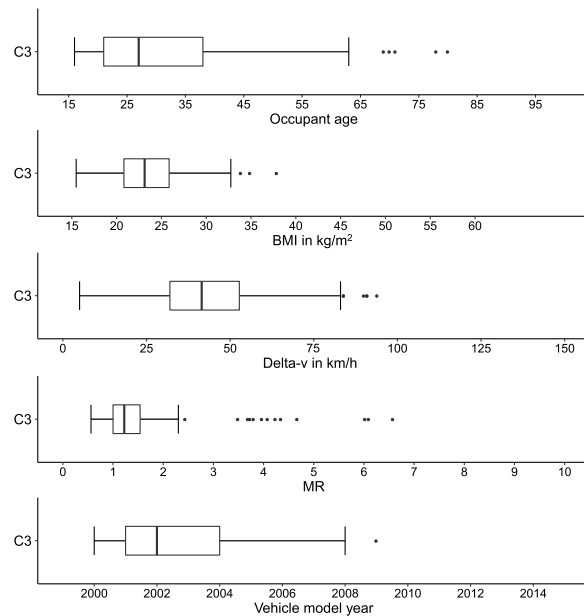


Fig. 6. Descriptive statistics on cluster 3 (C3 = 330).

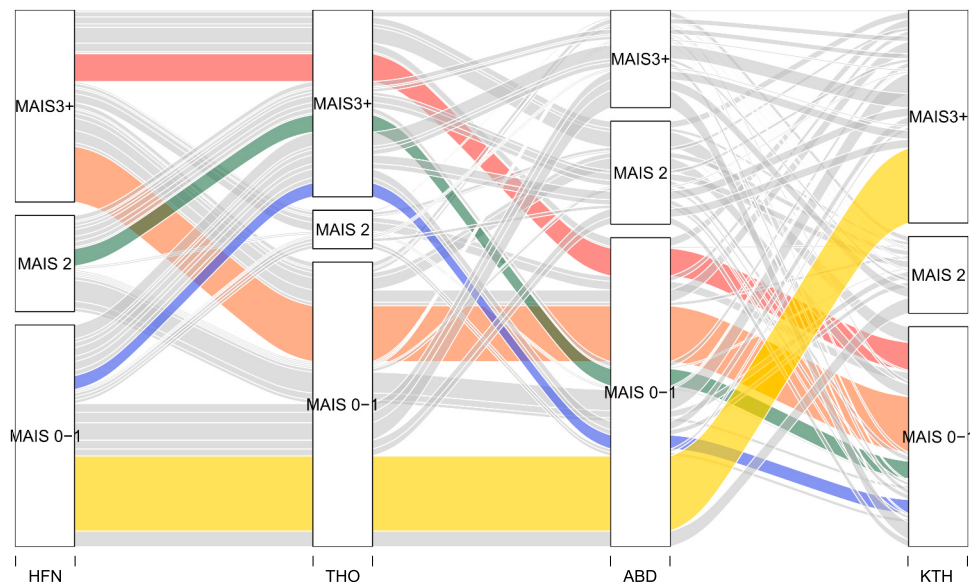


Fig. 7. Body region based injury patterns of seriously injured belted front row car occupants in cluster 3. Three levels of injury severity: MAIS 0–1, MAIS 2 and MAIS 3+. The size of the injury severity boxes and the width of the connecting curves are proportional to their frequency in cluster 3 (HFN: Head-Face-Neck, THO: Thorax, ABD: Abdomen, KTH: Knee-Thigh-Hip). For interpretation of the references to color in this figure citation, the reader is referred to the web version of this article.

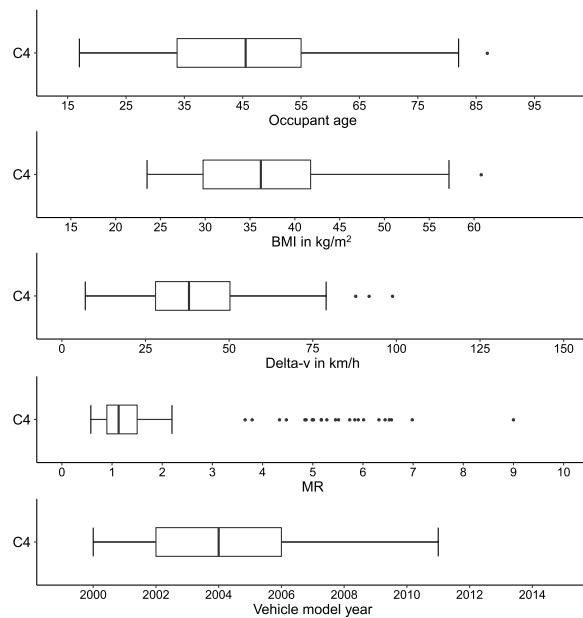


Fig. 8. Descriptive statistics on cluster 4 (C4 = 156).

frontal oblique crashes (22%) are the most frequent collision configurations in cluster 4. Collision opponents are presented in Table 3.

3.4. Cluster 5

Descriptive statistics for cluster 5 are shown in Fig. 10. The median occupant age in the cluster is 56 years old. 75% of the occupants had a BMI under 32 kg/m². The distributions of delta-v and MR show slightly lower values than in the data sample. Cluster 5 is the cluster with the newest vehicles compared to the other clusters. 50% of the vehicles are model year 2008 and onwards. As evident from Fig. 11 the thoracic region is the most severely injured body region for the occupants in this cluster. The majority of the occupants had a MAIS 3+ injury to the thorax without further injuries (blue). Some passengers sustained only a MAIS 3+ injury to the head (orange). Less frequent injury patterns in

common with the other clusters and the whole sample are displayed in yellow, red, dark green and gray. As indicated in Table 2, 30% of the collisions in this cluster were frontal oblique crashes, followed by frontal impacts with large overlap (22%) and moderate overlap (15%).

3.5. Cluster 6

The upper quartile of the occupant age in this cluster peaked at 79 years old. The median BMI is 26 kg/m². 75% of the cases had a delta-v under 37 km/h and the 50% had a MR under 1.1. The median model year is 2002 and 75% of the case vehicles are older than 2004. These facts are displayed in Fig. 12. MAIS 3+ injuries to the THO region, followed by the HFN region are the most common in this cluster (Fig. 13). A single MAIS 3+ thoracic injury is the most prevalent injury pattern (blue). Comparing the injury patterns in clusters 5 and 6 (Figs. 11 and

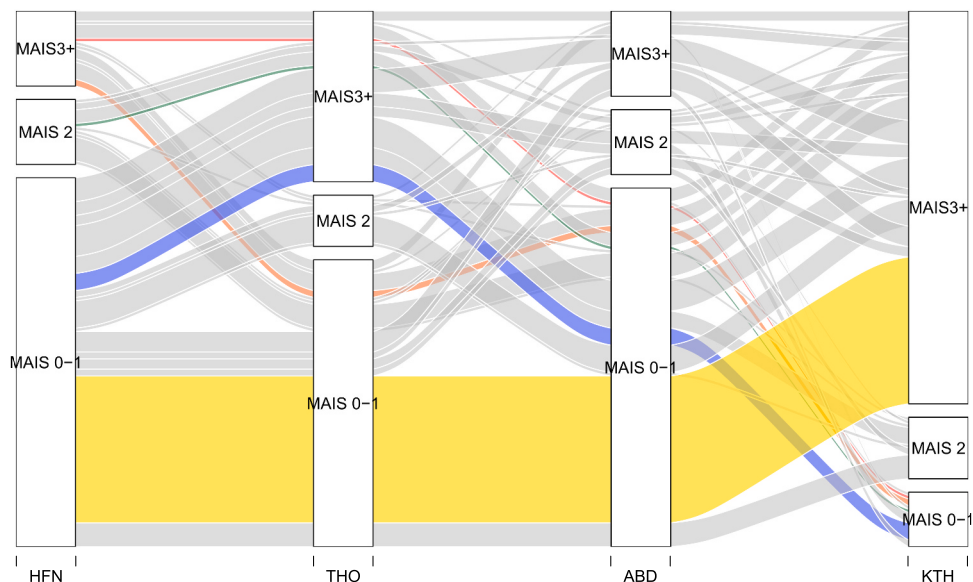


Fig. 9. Body region based injury patterns of seriously injured belted front row car occupants in cluster 4. Three levels of injury severity: MAIS 0–1, MAIS 2 and MAIS 3+. The size of the injury severity boxes and the width of the connecting curves are proportional to their frequency in cluster 4 (HFN: Head-Face-Neck, THO: Thorax, ABD: Abdomen, KTH: Knee-Thigh-Hip). For interpretation of the references to color in this figure citation, the reader is referred to the web version of this article.

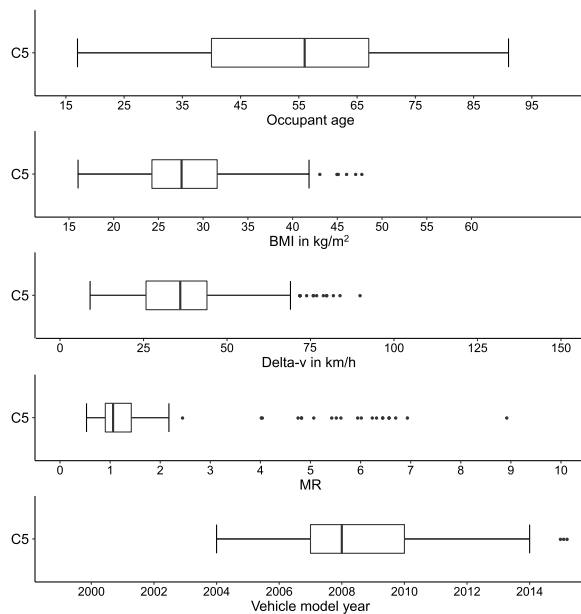


Fig. 10. Descriptive statistics on cluster 5 (C5 = 252).

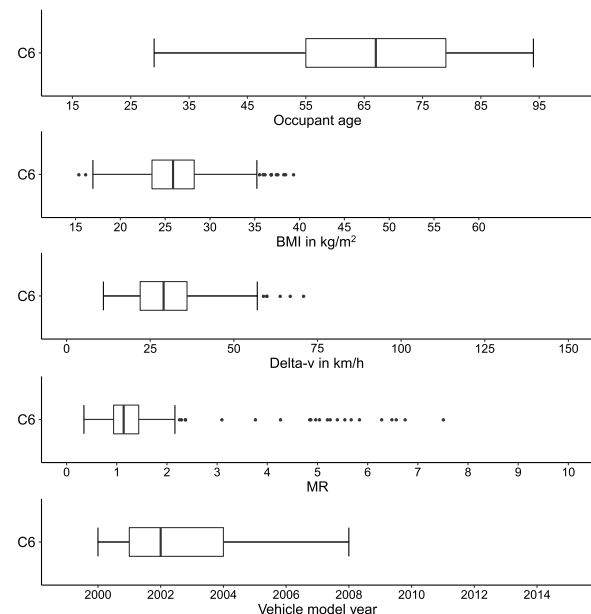


Fig. 12. Descriptive statistics on cluster 6 (C6 = 308).

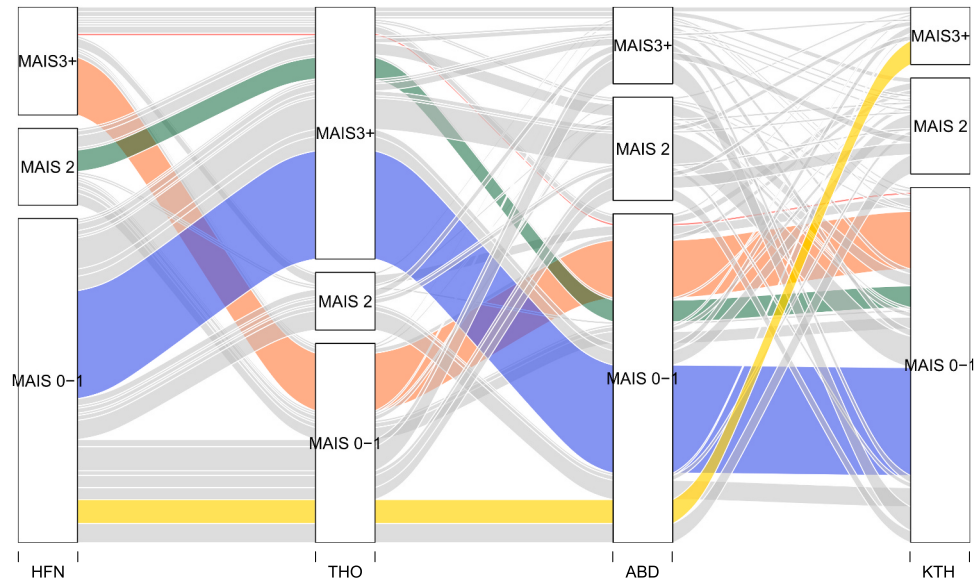


Fig. 11. Body region based injury patterns of seriously injured belted front row car occupants in cluster 5. Three levels of injury severity: MAIS 0–1, MAIS 2 and MAIS 3+. The size of the injury severity boxes and the width of the connecting curves are proportional to their frequency in cluster 5 (HFN: Head-Face-Neck, THO: Thorax, ABD: Abdomen, KTH: Knee-Thigh-Hip). For interpretation of the references to color in this figure citation, the reader is referred to the web version of this article.

13) shows that the proportion of serious thoracic and head injuries is larger in cluster 6, while severe abdominal injuries are more frequent in cluster 5. Some occupants cluster 6 sustained MAIS 3+ injuries to the HFN and to the THO region (red). This injury pattern is noticeably less frequent in cluster 5. According to Table 2 frontal oblique are the most prevalent collision configuration in cluster 6 with almost 40

4. Discussion

Other studies have applied machine learning techniques to accident data for the purpose of predicting injury severity (Iranitalab and Khatak, 2017; Theofilatos et al., 2019). This research is the first to apply unsupervised clustering algorithms to real-world crash data in order to identify injury patterns at the MAIS 3+ level that occur in the field

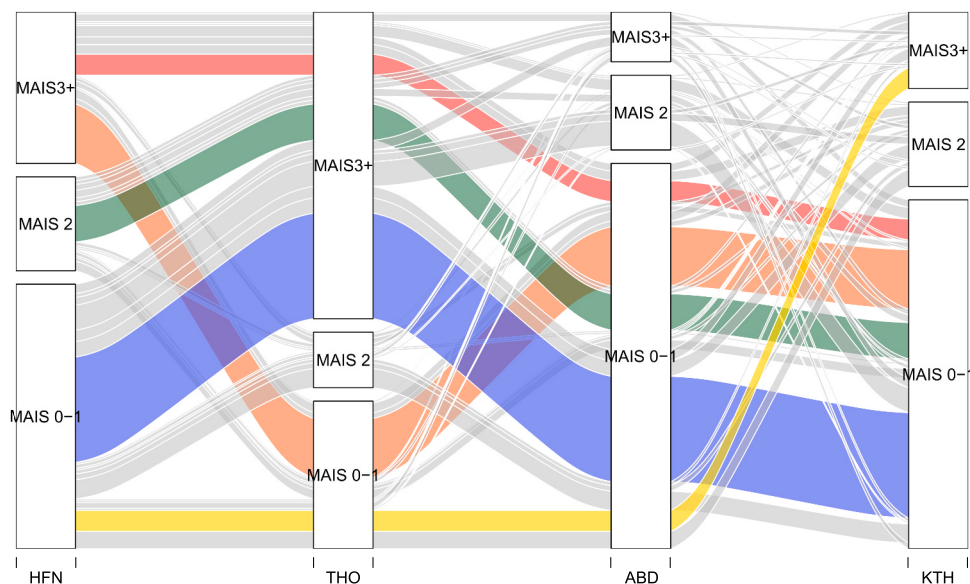


Fig. 13. Body region based injury patterns of seriously injured belted front row car occupants in cluster 6. Three levels of injury severity: MAIS 0–1, MAIS 2 and MAIS 3+. The size of the injury severity boxes and the width of the connecting curves are proportional to their frequency in cluster 6 (HFN: Head-Face-Neck, THO: Thorax, ABD: Abdomen, KTH: Knee-Thigh-Hip). For interpretation of the references to color in this figure citation, the reader is referred to the web version of this article.

despite current crashworthiness assessments without limiting the impact direction. The approach consisted of classifying seriously injured, belted occupants into clusters based on injured body regions, biomechanical characteristics and crash severity. Cluster analysis allowed the identification of six groups of occupants describing 77 % of the variability of the data set. The six resulting clusters and their main characteristics are presented in Fig. 3. Cases within five clusters (1, 3, 4, 5 and 6) were further analyzed in order to investigate which collision configurations caused the different injury patterns within the clusters. The associated collision configurations to each cluster are shown in Table 2. The type of collision opponent and its distribution within the clusters are indicated in Table 3.

Most of the cases in cluster 1 are young occupants who experienced a head-on collision with a fixed object. This group reveals a mass-compatibility issue, since the collision opponent was much heavier than the case vehicle. It is known from the literature that smaller vehicles are at disadvantage when crashing into a heavier vehicle or a rigid object (Hollowell and Gabler, 1996; Gabler and Hollowell, 1998; Zobel and Schwarz, 2001). Sustaining a MAIS 3+ injury to the KTH region as a single injury was the most common injury pattern in this cluster. The primary cause for KTH injuries in frontal collisions is the application of a force to the anterior surface of the flexed knee (Rupp et al., 2010). This force may be the result of intrusion and contact of the occupant's legs with the knee-bolster (Rupp et al., 2003). It is important to highlight that lateral collisions against pole-like objects are not frequent in either cluster 1 or in the whole sample. Electronic Stability Control (ESC) has been proven to reduce run-off-road crashes by 40% and single vehicle crashes by 25% (Høye, 2011). The reduction of skidding may be related to the reduction of lateral-pole impacts and the presence of frontal-pole crashes as a trade-off effect.

Cluster 3 contains younger occupants injured in vehicle-to-vehicle collisions. The collision configurations are equally distributed among

moderate overlap, frontal oblique and lateral oblique collisions. MAIS 3+ injuries to the head, thorax and KTH region are frequent in this cluster (see Fig. 7). Cluster 3 is the group with the highest proportion of MAIS 3+ abdominal injuries. Occupants in clusters 1 and 3 were involved in crashes with higher delta-v compared to the other clusters. However, few crashes in the data sample were above the delta-v values of the crashworthiness assessments. The 64 km/h of impact velocity in the IIHS (Insurance Institute for Highway Safety) moderate overlap crash test is equivalent to a delta-v of 70 km/h (Brumbelow, 2019). The quality and under-prediction of delta-v values in NASS-CDS has long been discussed, and some authors recommend the use of an EDR-based delta-v (Gabler et al., 2004; Hampton and Gabler, 2010; Stigson et al., 2012; Brumbelow, 2019). First, an EDR-based delta-v was not available for most of the crashes included this study. Second, this research covers many different collision types and configurations and hence, using the method proposed by Brumbelow et al. for predicting EDR-based delta-v would not be appropriate (Brumbelow, 2019).

Obesity is defined as a BMI equal to or greater than 30 kg/m². 75% of the seriously injured occupants in cluster 4 had a BMI greater than 30 kg/m². Most of these passengers in this cluster sustained a MAIS 3+ injury in the KTH region during a frontal impact. This fact causes difference in the appearance of the injury pattern plot (Fig. 9) when compared with the other clusters and the data sample. Rupp et al. proved with NASS-CDS data that an elevated BMI was associated with an increase in the risk of serious lower extremity injuries in frontal collisions (Rupp et al., 2013). MAIS 3+ thoracic injuries are the second most prevalent in cluster 4. Many studies have investigated the effect of obesity in abdominal injuries with NASS-CDS data. These injuries could be caused by poor safety belt positioning or submarining kinematics (Zarzaur and Marshall, 2008; Rupp et al., 2013; Poplin et al., 2015). None of these studies found an increased risk of abdominal injuries with higher BMI. Cluster 4 corroborates the results of the existing research.

Clusters 5 and 6 group the seriously injured elderly population in modern and older vehicles, respectively. Both data groups present similar characteristics and comparable injury patterns. MAIS 3+ injuries to the thorax without further injuries in the other body regions is the most common injury pattern in these clusters. The large number of severe thoracic injuries compared to the other body regions in clusters 5 and 6 contrasts to the other clusters. The increasing fragility of the thorax with age is an evident effect (Kent et al., 2005). Recent studies with NASS-CDS data have highlighted the presence of serious thorax injuries over other body regions in frontal impacts (Brumbelow, 2019; Forman et al., 2019). The values of the delta-v in cluster 5 (75% of the cases under 45 km/h), which consists predominantly of head-on collisions, may indicate that current crashworthiness assessments do not take into account thoracic injury in the elderly.

MAIS 3+ head and thoracic injuries decrease in cluster 5, while severe abdominal injuries increase, compared to cluster 6. The critical injury pattern of sustaining a MAIS 3+ HFN injury in combination with an MAIS 3+ THO injury is frequent in cluster 6 (colored in red in Fig. 13) but almost disappears in cluster 5. Forman et al. showed a reduction of AIS4+ injuries with newer vehicle model years with NASS-CDS data (Forman et al., 2019). The main differences between cluster 5 and cluster 6 are the vehicle model year and the associated collision configurations. Although frontal oblique is the most typical configuration in both clusters, cluster 5 tends more to frontal (with large overlap as second most prevalent configuration) and in cluster 6 lateral impact configurations predominate. Regarding the vehicle model year, there is a clear separation of the two clusters between the model years 2005 and 2007. In 2004, the IIHS started its side impact testing program in the US (Mueller et al., 2019). During this period curtain airbags began to be introduced as standard equipment in new vehicles. The reduction of serious HFN and THO injuries and the low presence of lateral collisions in cluster 5 (the cluster of the newer vehicles) provide evidence that improvements to the vehicle's side structure together with the introduction of the curtain airbag, as shown by Griffin et al. (2012) and Gaylor et al. (2018), have contributed to protect occupants from injury.

Oblique frontal impacts are the most prevalent collision configuration in the data sample of seriously injured belted occupants. This collision configuration and its effects on injury have already been studied (Bean et al., 2009; Rudd et al., 2011; Andricevic et al., 2018). NHTSA presented in 2012 a moving deformable barrier test procedure to evaluate oblique crashes, but this test has not been included in US NCAP yet (Saunders et al., 2012). The Federal Motor Vehicle Safety Standard (FMVSS) No. 208 includes a full-width crash test against a rigid wall at 30°, however this test still focuses on the protection of unbelted occupants.

4.1. Limitations

The use of the reconstruction delta-v in NASS-CDS is a limitation of this study. Also the assumption of 10,000 kg as the weight of the rigid objects for the calculation of the mass ratio in the cluster analysis has to be considered as a limitation. This assumption produces outliers in the distribution of the MR variable (Fig. 1). The cases considered in this study were not weighted with the NASS-CDS weights. This research focuses on the injury patterns of seriously injured occupants and the collision configurations in which they were involved. Since this study makes no comparison to lower severity crashes, the use of the NASS-CDS weighting factors is not necessary. However, it might be interesting for

further research to estimate the contribution of the clusters to the total number of seriously injured occupants in the US.

It is important to note that the clusters found in this study contain a large amount of information and research possibilities. The aim of this publication is to present the methodology and to provide insight into the current issues in severe real-world crashes without limiting the impact direction. Further work is planned on the validation of the clusters with a different accident database. Specific injuries and injury mechanisms related to the clusters are currently being investigated.

5. Conclusion

Unsupervised clustering algorithms have been applied to real-world crash data in order to classify seriously injured, belted occupants into clusters based on comparable injury patterns at the MAIS 3+ level, similar biomechanical characteristics and crash severity. To the knowledge of the authors, this is one of the first studies applying clustering to accident data and investigating serious-injury patterns without limiting the impact direction. The resulting clusters point out the current issues in the accident environment and represent new opportunities for vehicle safety. The key facts revealed in this study are:

- Oblique frontal impacts are the most prevalent collision configuration leading to serious injuries.
- MAIS 3+ thoracic injuries, especially in the elderly, occur more frequently in the field than injuries to other body regions.
- Frontal pole impacts, generally in configurations with moderate overlap, are common in the accident environment causing severe injuries to the thorax and Knee-Thigh-Hip regions in the younger population.
- Lateral pole impacts are rarely found in the sample of seriously injured occupants.
- MAIS 3+ injuries to the Knee-Thigh-Hip region have been observed in obese occupants in frontal collisions.
- The presence of severely injured occupants in lateral collisions decreased with newer vehicle model years.
- The introduction of curtain airbags and improvements to the vehicle's side structure have contributed to protect occupants from serious head and thoracic injuries.

Authors' contribution

Rocio Suarez del Fueyo: term, data curation, investigation, methodology, formal analysis, software and writing – original draft. Mirko Junge: resources, visualization, conceptualization, supervision, writing – review and editing. Francisco Lopez-Valdes and Clay Gabler: conceptualization, supervision, writing – review and editing. Lukas Wörner: project administration, supervision, writing – review and editing. Stefan Hiermaier: supervision, writing – review and editing.

Declaration of Competing Interest

The authors declare that they have no known competing financial interests or personal relationships that could have appeared to influence the work reported in this paper.

Appendix A

Table 4
PCA results including the proportion of variance defined by each component.

	PC1	PC2	PC3	PC4	PC5	PC6	PC7	PC8	PC9
Standard deviation	1.28	1.17	1.06	0.99	0.96	0.93	0.87	0.84	0.77
Variance	0.18	0.15	0.12	0.11	0.09	0.09	0.08	0.08	0.07
Cumulative variance	0.18	0.33	0.46	0.57	0.67	0.77	0.85	0.93	1.00

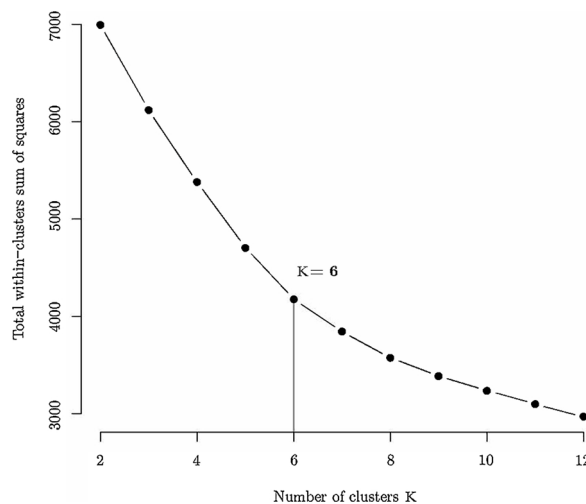


Fig. 14. Recommended number of clusters ($K = 6$) after the elbow method.

References

- AAAM, 1998. Abbreviated Injury Scale; 1990 Revision: Update 98. Association for the Advancement of Automotive Medicine (AAAM).
- AAAM, 2008. Abbreviated Injury Scale; 2005 Revision: Update 2008. Association for the Advancement of Automotive Medicine (AAAM).
- Andricovic, N., Junge, M., Krampe, J., 2018. Injury risk functions for frontal oblique collisions. *Traff. Inj. Prev.* 19 (5), 518–522.
- Arbogast, K.B., Durbin, D.R., Kallan, M.J., Elliott, M.R., Winston, F.K., 2005. Injury risk to restrained children exposed to deployed first- and second-generation air bags in frontal crashes. *Arch. Pediatr. Adolesc. Med.* 159 (4), 342–346.
- Baker, S.P., O'Neill, B., Haddon Jr., W., Long, W.B., 1974. The injury severity score: a method for describing patients with multiple injuries and evaluating emergency care. *J. Trauma Acute Care Surg.* 14 (3), 187–196.
- Bean, J.D., Kahane, C.J., Mynatt, M., Rudd, R.W., Rush, C.J., Wiacek, C., 2009. Fatalities in Frontal Crashes Despite Seat Belts and Air Bags—Review of All CDS Cases—Model and Calendar Years 2000–2007–122 Fatalities (Tech. Rep.). US DOT: NHTSA (Report No. DOT HS 811 202).
- Brumbelow, M.L., 2019. Front crash injury risks for restrained drivers in good-rated vehicles by age, impact configuration, and EDR-based delta V. Proceedings of the 2019 International IRCOBI Conference on the Biomechanics of Injury – Florence, Italy.
- Brumbelow, M.L., Mueller, B.C., Arbelaez, R.A., 2015. Occurrence of serious injury in real-world side impacts of vehicles with good side-impact protection ratings. *Traff. Inj. Prev.* 16 (1), S125–S132.
- Brumbelow, M.L., Zuby, D.S., 2009. Impact and injury patterns in frontal crashes of vehicles with good ratings for frontal crash protection. 21st Experimental Safety Vehicle Conference (ESV) – Stuttgart, Germany.
- Crandall, C.S., Olson, L.M., Sklar, D.P., 2001. Mortality reduction with air bag and seat belt use in head-on passenger car collisions. *Am. J. Epidemiol.* 153 (3), 219–224.
- Elvik, R., Vaa, T., Hoye, A., Sorensen, M., 2004. Factors contributing to road accidents. In: Elvik, R., Hoye, A., Vaa, T., Sorensen, M. (Eds.), *The Handbook of Road Safety Measures*. Emerald Group Publishing Limited, Oxford, pp. 29–79.
- Forman, J., Poplin, G.S., Shaw, C.G., McMurry, T.L., Schmidt, K., Ash, J., Sunneveng, C., 2019. Automobile injury trends in the contemporary fleet: belted occupants in frontal collisions. *Traff. Inj. Prev.* 20 (6), 607–612.
- Gabler, H.C., Hampton, C.E., Hinch, J., 2004. Crash severity: A comparison of event data recorder measurements with accident reconstruction estimates. *SAE World Congress* (No. 2004-01-1194).
- Gabler, H.C., Hollowell, W.T., 1998. The aggressivity of light trucks and vans in traffic crashes. *SAE Trans.* 1444–1452.
- Gabler, H.C., Weaver, A.A., Stitzel, J.D., 2015. Automotive field data in injury biomechanics. In: Yoganandan, N., Nahum, A.M., Melvin, J.W. (Eds.), *Accidental Injury – Biomechanics and Prevention*. Springer, New York.
- Gaylor, L., del Fueyo, R.S., Junge, M., 2016. Crashworthiness improvements of the vehicle fleet. *IRCOBI Conference Proceedings* – Malaga, Spain 592–605.
- Gaylor, L., Junge, M., Abaneriba, S., 2018. Thoracic side airbags and structural performance in vehicle-vehicle lateral impacts. *Int. J. Crashworthiness* 23 (1), 108–116.
- Glassbrenner, D., 2012. An Analysis and of Recent and Improvements to Vehicle and Safety (Tech. Rep.). US DOT: NHTSA (Report No. DOT HS 811 572).
- Griffin, R., Huisings, C., McGwin Jr., G., Reiff, D., 2012. Association between side-impact airbag deployment and risk of injury: a matched cohort study using the CIREN and the NASS-CDS. *J. Trauma Acute Care Surg.* 73 (4), 914–918.
- Hackney, J., Quarles, V., 1982. The New Car Assessment Program – status and effect. 9th Experimental Safety Vehicle Conference (ESV) – Kyoto, Japan 809–824.
- Hampton, C.E., Gabler, H.C., 2010. Evaluation of the accuracy of nass/cds delta-v estimates from the enhanced Winsmash algorithm. *Annals of Advances in Automotive Medicine/Annual Scientific Conference*, Vol. 54 241.
- Hartigan, J.A., Wong, M.A., 1979. Algorithm AS 136: a k-means clustering algorithm. *J. R. Stat. Soc. Ser. C Appl. Stat.* 28 (1), 100–108.
- Hollowell, W.T., Gabler, H.C., 1996. NHTSA's vehicle aggressivity and compatibility research program. 15th Experimental Safety Vehicle Conference (ESV) – Melbourne, Australia.
- Hoye, A., 2011. The effects of Electronic Stability Control (ESC) on crashes – an update. *Accid. Anal. Prev.* 43 (3), 1148–1159.
- Iranitalab, A., Khattak, A., 2017. Comparison of four statistical and machine learning methods for crash severity prediction. *Accid. Anal. Prev.* 108, 27–36.
- Kahane, C.J., 2015. Lives Saved by Vehicle Safety Technologies and Associated Federal Motor Vehicle Safety Standards, 1960 to 2012–Passenger Cars and LTVs – with Reviews of 26 FMVSS and the Effectiveness of Their Associated Safety Technologies in Reducing Fatalities, Injuries, and Crashes (Tech. Rep.). US DOT: NHTSA (Report No. DOT HS 812 069).
- Kassambara, A., 2017. Practical Guide to Cluster Analysis in R: Unsupervised Machine Learning. STHDA.
- Kent, R., Lee, S.-H., Darvish, K., Wang, S., Poster, C.S., Lange, A.W., Matsuoka, F., 2005. Structural and material changes in the aging thorax and their role in crash protection for older occupants. *Stapp Car Crash J.* 49, 231–249.
- Kleinberger, M., Sun, E., Eppinger, R., Kuppa, S., Saul, R., 1998. Development of improved injury criteria for the assessment of advanced automotive restraint systems. *NHTSA Docket 4405* (9), 12–17.
- Kodinariya, T.M., Makwana, P.R., 2013. Review on determining number of cluster in k-means clustering. *Int. J. Adv. Res. Comput. Sci. Manag. Stud.* 1 (1), 90–95.

- Lopez-Valdes, F.J., Lau, A., Lamp, J., Riley, P., Lessley, D., Damon, A., Kent, R., 2010. Analysis of spinal motion during frontal impacts. comparison between PMHS and ATD. *Ann. Adv. Autom. Med./Annual Scientific Conference* 54, 61–78.
- Lopez-Valdes, F.J., Mroz, A., Eggers, B., Pipkorn, B., Muehlbauer, S., Schick, S., Peldschus, S., 2019. Chest injuries of elderly post mortem human surrogates (PMHS) under seat belt and airbag loading in frontal sled impacts. comparison to matching THOR tests. *Traff. Inj. Prev.* 19, S55–S63.
- MacQueen, J., 1967. Some methods for classification and analysis of multivariate observations. *Proceedings of the FIFTH BERKELEY SYMPosium on Mathematical Statistics and Probability*, Vol. 1 281–297.
- Mueller, B.C., Arbelaez, R.A., Brumbelow, M.L., Nolan, J.M., 2019. Comparison of higher severity side impact tests of IIHS-good-rated vehicles struck by LTIVs and a modified IIHS barrier with the current IIHS side test and real-world crashes. *26th Experimental Safety Vehicle Conference (ESV)* – Eindhoven, Netherlands.
- NHTSA, 2010. National Automotive Sampling System (NASS) Crashworthiness Data System – Analytical User's Manual 2009 (Tech. Rep.). US DOT: National Center for Statistics and Analysis. US Dept. of Transportation, Washington, DC, 1, pp. 1–155.
- Niebuhr, T., Junge, M., Achmus, S., 2013. Pedestrian injury risk functions based on contour lines of equal injury severity using real world pedestrian/passenger-car accident data. *Annual Proceedings of the Association for the Advancement of Automotive Medicine (AAAM)*, Vol. 57 145–154.
- Niebuhr, T., Junge, M., Achmus, S., 2015. Expanding pedestrian injury risk to the body region level: How to model passive safety systems in pedestrian injury risk functions. *Traff. Inj. Prev.* 16 (5), 519–531.
- Niebuhr, T., Junge, M., Rosen, E., 2016. Pedestrian injury risk and the effect of age. *Accid. Anal. Prev.* 86, 121–128.
- O'Neill, B., 2009. Preventing passenger vehicle occupant injuries by vehicle design – a historical perspective from IIHS. *Traff. Inj. Prev.* 10 (2), 113–126.
- Osler, T., Baker, S.P., Long, W., 1997. A modification of the injury severity score that both improves accuracy and simplifies scoring. *J. Trauma Acute Care Surg.* 43 (6), 922–926.
- Parent, D., Craig, M., Moorhouse, K., 2017. Biofidelity evaluation of the THOR and Hybrid III 50 th percentile male frontal impact anthropomorphic test devices. *Stapp Car Crash J.* 61, 227–276.
- Pearson, K., 1901. Principal components analysis. *Lond. Edinb. Dublin Phil. Mag. J. Sci.* 6 (2), 559.
- Poplin, G.S., McMurry, T.L., Forman, J.L., Hartka, T., Park, G., Shaw, G., Crandall, J., 2015. Nature and etiology of hollow-organ abdominal injuries in frontal crashes. *Accid. Anal. Prev.* 78, 51–57.
- Radja, G.A., 2016. National Automotive Sampling System-Crashworthiness Data System, 2015 Analytical User's Manual (Tech. Rep.). US DOT: NHTSA.
- Rhule, H., Moorhouse, K., Donnelly, B., Stricklin, J., 2009. Comparison of WorldSID and ES-2re biofidelity using an updated biofidelity ranking system. *21st Experimental Safety Vehicle Conference (ESV)* – Stuttgart, Germany.
- Rudd, R., Scarboro, M., Saunders, J., 2011. Injury analysis of real-world small overlap and oblique frontal crashes. *22nd Experimental Safety Vehicle Conference (ESV)* – Washington, DC, USA.
- Rupp, J.D., Flannagan, C.A., Kuppa, S.M., 2010. Injury risk curves for the skeletal knee-thigh-hip complex for knee-impact loading. *Accid. Anal. Prev.* 42 (1), 153–158.
- Rupp, J.D., Flannagan, C.A., Leslie, A.J., Hoff, C.N., Reed, M.P., 2013. Effects of BMI on the risk and frequency of AIS 3+ injuries in motor-vehicle crashes. *Obesity* 21 (1), E88–E97.
- Rupp, J.D., Reed, M.P., Jeffreys, T.A., Schneider, L.W., 2003. Effects of hip posture on the frontal impact tolerance of the human hip joint. *Stapp Car Crash J.* 47, 21–33.
- Saunders, J., Craig, M., Parent, D., 2012. Moving deformable barrier test procedure for evaluating small overlap/oblique crashes. *SAE Int. J. Commercial Vehic.* 5 (2012-01-0577), 172–195.
- Seacrist, T., Balasubramanian, S., Garcia-Espana, F., Maltese, M., Lopez-Valdes, F.J., Kent, R.K.A., 2010. Kinematic comparison of pediatric human volunteers and the Hybrid-III 6-year-old Anthropomorphic Test Device. *Ann. Adv. Autom. Med./Annual Scientific Conference* 54, 97–108.
- Segui-Gomez, M., Lopez-Valdes, F.J., 2012. Injury severity measurements and survival outcome. In: Baker, S., Li, G. (Eds.), *Injury Research: Theories, Methods and Approaches*, 1st ed. Springer.
- Segui-Gomez, M., Lopez-Valdes, F.J., Crandall, J.R., 2009. Characterizing the distribution of injury and injury severity for belted front seat occupants involved in frontal crashes. *Proceedings of the 2019 International Ircobi Conference on the Biomechanics of Injury* – York, United Kingdom.
- Segui-Gomez, M., Lopez-Valdes, F.J., Frampton, R., 2010. Real-world performance of vehicle crash test: the case of EuroNCAP. *Injury Prev.* 16 (2), 101–106.
- Stevens, S.S., 1946. On the theory of scales of measurement. *Science* 103 (2684), 677–680.
- Stigson, H., Kullgren, A., Rosén, E., 2012. Injury risk functions in frontal impacts using data from crash pulse recorders. *Annual Proceedings of the Association for the Advancement of Automotive Medicine (AAAM)*, Vol. 56 267–276.
- Theofilatos, A., Chen, C., Antoniou, C., 2019. Comparing machine learning and deep learning methods for real-time crash prediction. *Transp. Res. Rec.* 2673 (8), 169–178.
- van Ratingen, M., Williams, A., Lie, A., Seeck, A., Castaing, P., Kolke, R., Miller, A., 2016. The European New Car Assessment Programme: a historical review. *Chin. J. Traumatol.* 19 (2), 63–69.
- Zarza, B.L., Marshall, S.W., 2008. Motor vehicle crashes obesity and seat belt use: a deadly combination? *J. Trauma Acute Care Surg.* 64 (2), 412–419.
- Zhang, F., Chen, C.L., 2013. NASS-CDS: Sample Design and Weights (Tech. Rep.). US DOT: NHTSA.
- Zobel, R., Schwarz, T., 2001. Development of criteria and standards for vehicle compatibility. *17th Experimental Safety Vehicle Conference (ESV)* – Amsterdam.